

Reconstruction of charged Kaons and $\phi(1020)$ in Ag+Ag collisions at $\sqrt{s_{NN}} = 2.55$ GeV with HADES

Marvin Kohls^{1,*} for the HADES Collaboration

¹Institut für Kernphysik, Goethe University Frankfurt am Main

Abstract. In March 2019, the HADES collaboration recorded $13.7 \cdot 10^9$ Ag(1.58A GeV)+Ag events as part of the FAIR Phase-0 program. The analysis steps necessary to extract the phase space information for K^+ , K^- and $\phi(1020)$ are presented in this proceeding.

1 Introduction

The **H**igh **A**cceptance **D**i**E**lectron **S**pectrometer (HADES) is a fixed target experiment connected to the SIS18 synchrotron at GSI in Darmstadt. SIS18 can accelerate heavy ion beams to kinetic energies of up to 2 GeV per nucleon. This realizes center of mass energies of $\sqrt{s_{NN}} \approx 2 - 3$ GeV.

The energetically most favourable process for strange hadron production is the reaction $NN \rightarrow N\Lambda K$ with a threshold energy of 2.55 GeV, leading to the creation of a K^+/K^0 and a Λ^0 . Hence, at the investigated collision energy of $\sqrt{s_{NN}} = 2.55$ GeV strangeness is either produced at or below the elementary production threshold. As a consequence, the production of strangeness is driven by collective effects of the created medium rather than isolated NN collisions.

Furthermore, the evaluation of density distributions within neutron star mergers and heavy ion collisions shows comparable values [1]. Consequently, investigating heavy ion collisions at low energies and high baryochemical potentials offers a probe for otherwise purely astronomical events. In particular, it allows the investigation of the microscopic composition of dense nuclear matter, which is hardly possible in astronomical observations. The observed steep rise of their excitation function makes the K^\pm and ϕ yield a sensitive probe for the properties of the created medium.

2 The HADES Experiment

The spectrometer setup during the measurement of Ag+Ag collisions at $\sqrt{s_{NN}} = 2.55$ GeV is depicted in Figure 1. Due to the forward boost of secondary particles resulting from the fixed target configuration, the detectors are all situated in the forward direction in the laboratory reference frame.

In the azimuthal direction, the detector setup reaches a nearly total 360° coverage. A range between approximately 18° and 85° is covered in the polar angle direction. This corresponds to a proton rapidity coverage between -0.65 to 0.5 in the center of mass system.

*e-mail: m.kohls@gsi.de

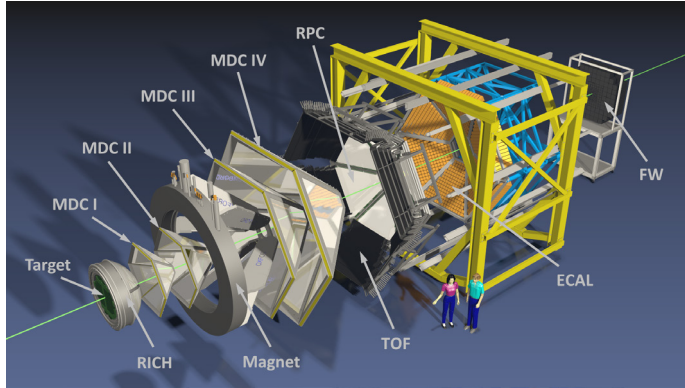


Figure 1. The HADES detector setup during the Ag+Ag beamtime in March 2019 stretched along the beam axis to illustrate the individual subdetectors.

In front of the target, a diamond-based t_0 detector is situated, registering the starting time for each reaction. Afterwards, **M**ultiwire **D**rift **C**hambers (MDCs) form four layers of Ar/CO₂ gas-filled detection volumes with six stereo layers of sensing wires each. With the toroidal magnet between layers II and III, the MDCs perform the charged particle tracking and energy loss measurement before and after the magnetic field. The MDCs are followed by the TOF and **R**esistive **P**late **C**hamber (RPC) time of flight wall, usually referred to as **M**ultiplicity and **E**lectron **T**rigger **A**rray (META) detectors. TOF consists of 384 scintillation rods, so energy loss measurements are possible. META also functions as a trigger for the event multiplicity. More details on the setup can be found in [2].

With the META time of flight information and the bent trajectory reconstructed by the MDCs, the p/q of a particle can be determined. Together with the energy loss information, these are designated PID criteria.

The **R**ing **I**maging **C**herenkov **D**etector (RICH) and the **E**lectromagnetic **C**alorimeter (ECal) are not used in this analysis. RICH is used for the identification of leptons via the produced Cherenkov light. ECal detects and aids in identifying leptons, π^\pm and photons. The **F**orward **W**all (FW) in return registers the spectators of the collision in order to determine the event plane.

3 Analysis

As the production of charged Kaons and ϕ -mesons happens at (K^+) or below (K^-, ϕ) the free NN production threshold, the corresponding particle multiplicities are orders of magnitude below those of protons, π^\pm and light nuclei.

As a consequence, not only track quality criteria are used to increase the significance of the K^\pm signals but also the MDC and TOF energy loss information to suppress the p and π^\pm contributions in the mass spectra. In order to obtain the true signal from the particle spectra, the background is interpolated (K^\pm) below the peak or estimated by the event mixing technique (ϕ) and then subtracted. This is performed for all mass spectra in the corresponding $(m_t - m_0)$ - y intervals, as indicated on the left side of Figure 2, where the mass (K^\pm) and invariant mass (ϕ) spectra (black) and the corresponding background estimation (red) are displayed. In total about 1.34×10^7 K^+ , 1.21×10^5 K^- and 5.67×10^3 ϕ could be reconstructed for differential analyses. For the K^+ mass spectrum the tails of the π^+ and proton mass distributions overlap with the signal and rise steeply towards the edges of the spectra. Similarly the

π^- mass tail overlaps with the K^- mass spectrum. The apparent difference in mass resolution between K^+ and K^- results from the mass spectra being taken from RPC (K^+) and TOF (K^-), which possess a different timing resolution.

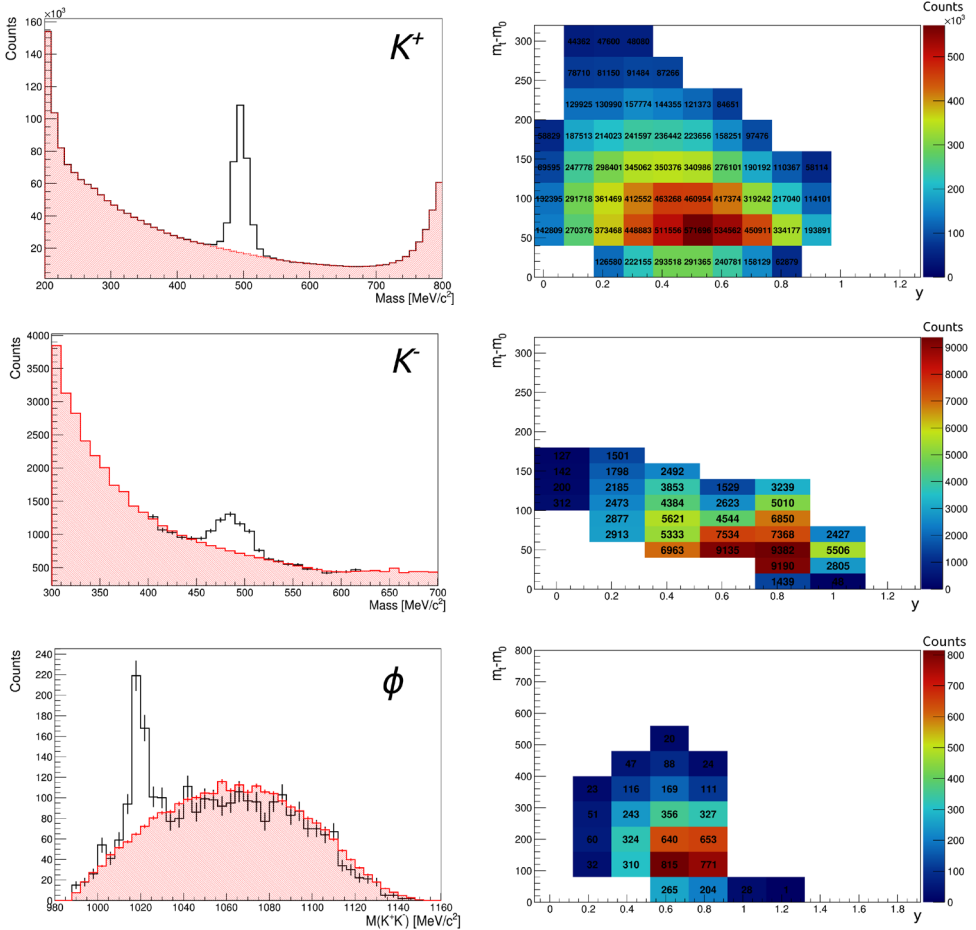


Figure 2. Exemplary differential mass spectra for K^+ , K^- and ϕ (left) and the resulting reconstructed phase space (right) in 0 – 30% centrality. The full collection of spectra can be found in [2].

This results in a measured (raw) yield map of the particles’ phase space, as displayed on the right side of Figure 2. The distribution has to be corrected for loss in geometrical acceptance and tracking as well as identification efficiency. UrQMD [3] generated events are transported through a GEANT representation of the HADES detector setup to obtain the relative loss due to those effects. This relative loss is used to correct the reconstructed yield in each phase space bin, resulting in the final $(m_t - m_0)$ spectra for each rapidity interval. More details on the procedure can be found in [2].

The obtained spectra are fitted by a double isotropic statistical distribution [4]

$$\left(\frac{d^2N}{dm_t dy} \right)_{DIS} = \left(\frac{d^2N}{dm_t dy} \right)_{IS} (m_t, y - \eta) + \left(\frac{d^2N}{dm_t dy} \right)_{IS} (m_t, y + \eta) \quad (1)$$

which is the superposition of two radially symmetric thermal sources of the form

$$\frac{d^2N}{dm_t dy} = 2\pi \cdot C \cdot \cosh(y) \cdot e^{-\frac{m_t \cosh(y)}{T_{\text{Eff}}}} \quad (2)$$

each with a distance η to the centre of mass rapidity. The superposition is motivated by the generally non-spherical nature of the collision system. Summing over the available data and integrating the fitted function to extrapolate the yield in the uncovered phase space region, one obtains a final integrated yield for each rapidity interval. Plotting the particle production yield as a function of rapidity, a dN/dy distribution is obtained. Integrating equation 2 over dm_t and fitting the resulting superimposed function onto the dN/dy distribution is used to describe the unmeasured phase space region for the total production yield per event. Besides the yield, T_{Eff} can also be extracted from the fit function for every rapidity bin and will be presented in an upcoming publication.

4 Outlook

This analysis aims to investigate previous results like the observed steep rise of the ϕ/K^- [5], and the ϕ/Ξ^- [6] ratio towards low collision energies. Furthermore, we aim to check the universal scaling of strange hadron production yields according to $\text{Mult}/\langle A_{\text{part}} \rangle \propto \langle A_{\text{part}} \rangle^\alpha$ as observed in [6] and [5]. In [5] it is found as well, that the lower T_{Eff} for the K^- can be explained by feed-down from the $\phi \rightarrow K^+ K^-$ channel, which will also be investigated.

Lastly, direct comparisons of HADES results to existing data and hadronic transport models like UrQMD [3] and SMASH [7] as well as thermal models, like presented in [8], will be performed.

References

- [1] J. Adamczewski-Musch, J., Arnold, O., Behnke, C. et al., **Nat. Phys.** **15**, 1040–1045 (2019)
- [2] M. Kohls, *Reconstruction and Analysis of Charged Kaons and ϕ -Mesons from Ag+Ag-Collisions at 1.58 AGeV*, PhD Thesis, Goethe University Frankfurt, to be published
- [3] S. A. Bass, M. Belkacem, M. Bleicher, M. Brandstetter, L. Bravina, C. Ernst, L. Gerland, M. Hofmann, S. Hofmann and J. Konopka, et al., **Prog. Part. Nucl. Phys.** **41** (1998), 255-369
- [4] S. Spies, *Strange hadron production in Ag+Ag collisions at 1.58A GeV*, PhD Thesis, Goethe University Frankfurt, 2022
- [5] H. Schuldes [HADES], **Nucl. Phys. A** **967** (2017), 804-807
- [6] M. S. Abdallah et al. [STAR], **Phys. Lett. B** **831** (2022), 137152
- [7] H. Petersen, D. Oliinychenko, M. Mayer, J. Staudenmaier and S. Ryu, **Nucl. Phys. A** **982** (2019), 399-402
- [8] S. Harabasz, W. Florkowski, T. Galatyuk, M. Gumberidze, R. Ryblewski, P. Salabura and J. Stroth, **Phys. Rev. C** **102** (2020) no.5, 054903